AD-A094 281 SOUTHEASTERN MASSACHUSETTS UNIV NORTH DARTMOUTH DEPT --ETC F/G 12/1
SOME EXPERIMENTAL RESULTS ON LINEAR ESTIMATION FOR IMAGE ANALYS--ETC(U)
JAN 81 C H CHEN, R WU, C YEN N00014-79-C-0494
UNCLASSIFIED SMU-EE-TR-81-4 NL

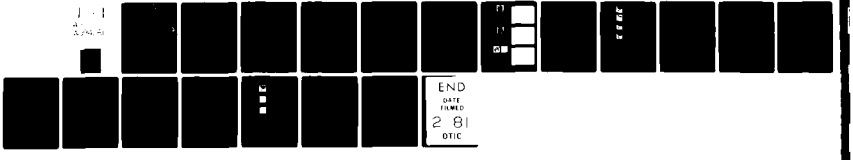

END
DATE FILMED
2 81
DTIC

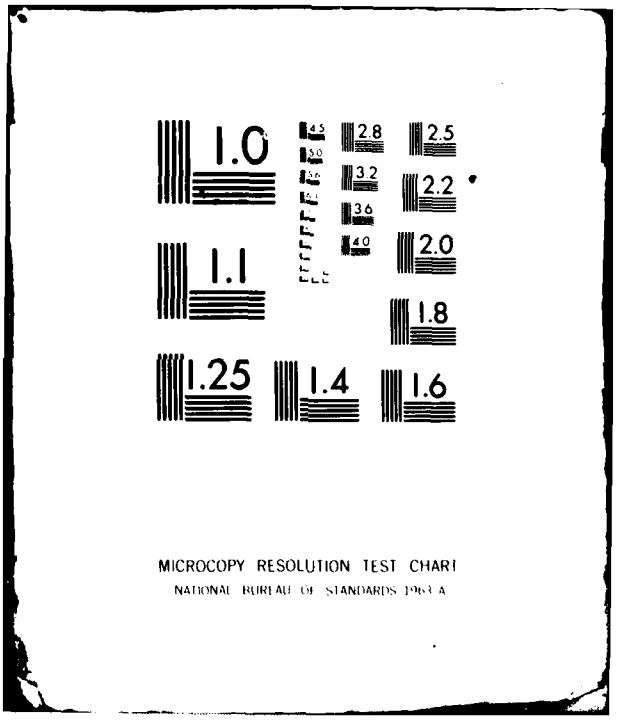
1.0
1.1
1.25
1.4
1.6
1.8
2.0
2.2
2.5
2.8
3.2
3.6
4.0
MICROCOPY RESOLUTION TEST CHART
NATIONAL BUREAU OF STANDARDS 1963-A

Technical Report
Contract Number N00014-79-C-0494
SMU-EE-TR-81-4
January 28, 1981

SOME EXPERIMENTAL RESULTS ON LINEAR ESTIMATION FOR IMAGE ANALYSIS*

BY
C. H. Chen
Rong-Hwang Wu
Chihsung Yen
Department of Electrical Engineering
Southeastern Massachusetts University
North Dartmouth, Massachusetts 02747

*The support of the Statistics and Probability Program of the Office of Naval Research on this work is gratefully acknowledged.

SOME EXPERIMENTAL RESULTS ON LINEAR ESTIMATION FOR IMAGE ANALYSIS

C. H. Chen
Rong-Hwang Wu
Chihsung Yen

1. Introduction

In a previous report (ref. 1), a critical comparison is made on the various statistical image segmentation techniques. Linear estimation plays an important role in image segmentation which may be considered as an estimation problem. Included in the linear estimation methods considered in Ref. 1 are the parameter estimation for ARMA models, Fisher's linear discriminant, maximum likelihood and maximum a posteriori estimations for the regions, boundary estimation via split-and-merge algorithm, and decision-directed estimation using conditional population-mixture model. In this report, experimental results are presented for a textured subimage on the segmentation by maximum likelihood estimation, maximum a posteriori estimation, and Fisher's linear discrimant. Among the three methods, the maximum a posteriori estimation performs the best with 3.96% segmentation error, the Fisher's linear discriminant is a close second with 4.6% segmentation error and requires slightly more computation. The performance of the maximum likelihood estimation is much worse even though it requires less computation than the other two methods.

2. Construction of the Textured Subimage

The construction of the 64x64 textured subimage was kindly described by Dr. Charles W. Therrien of MIT Lincoln Laboratory who employed the textured subimage in his study of the linear filtering

models for image segmentation and classification (Ref. 2). The desired subimage is constructed from subimages 5 and 9 (counting from upper left to lower right horizontally) of image B2568-38 of USC data base by using the following procedure. For each point (n,m), the following expressions are evaluated.

$$B1(n, m) = (n-36) + (m-40)^2/50$$

$$B2(n, m) = ((n-48)/8)^2 + ((m-20)/12)^2 - 1$$

Then if

$B1 < 0$ or $B2 < 0$, take point from subimage 5

if $B1 > 0$ and $B2 > 0$, take point from subimage 9

This results in a new subimage with the texture from subimage 5 above the parabolic boundary and within the elipse and the texture from subimage 9 everywhere else. The texture from subimage 5 is denoted as type 1 while the texture from subimage 9 is denoted as type 2. Thus the segmentation is to classify for each pixel whether it is from the type 1 or from the type 2 texture. For the results in Ref. 2, the filters were 4x4 causal (first quadrant) computed by solving two-dimensional normal equations with an estimated correlation function. Transition probabilities computed in the paper made use of 5x5 neighborhoods.

By using the lineprinter display with 16 levels, Fig. 1a, 1b and 1c show respectively the original subimages 5, 9 and the constructed subimage. Two-level displays of these subimages from the Tektronix 4010 terminal are shown in Fig. 2. Fig. 3 shows the ideal segmentation as defined by the parabola and elipse in the above quations.

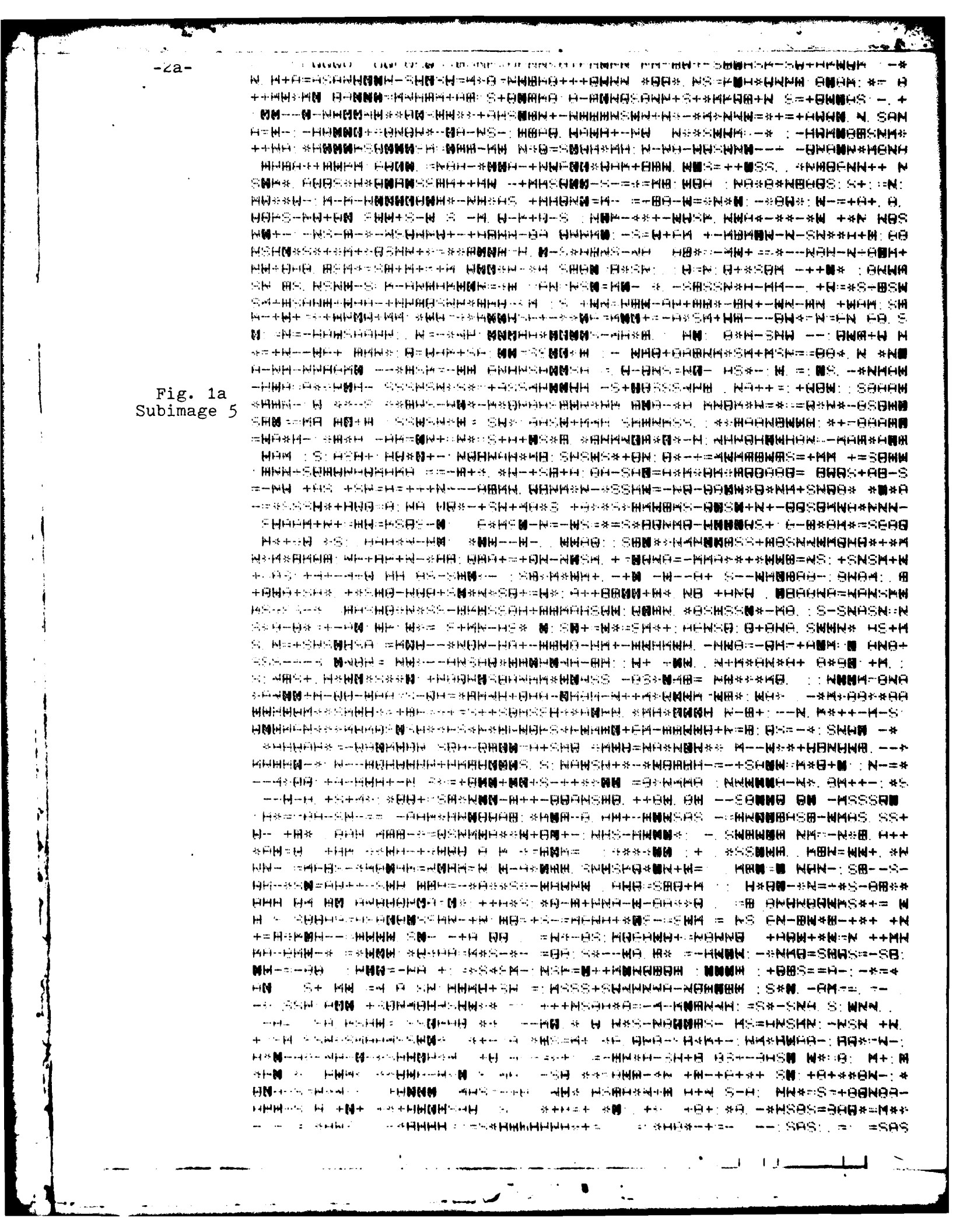

Fig. 1a
Subimage 5

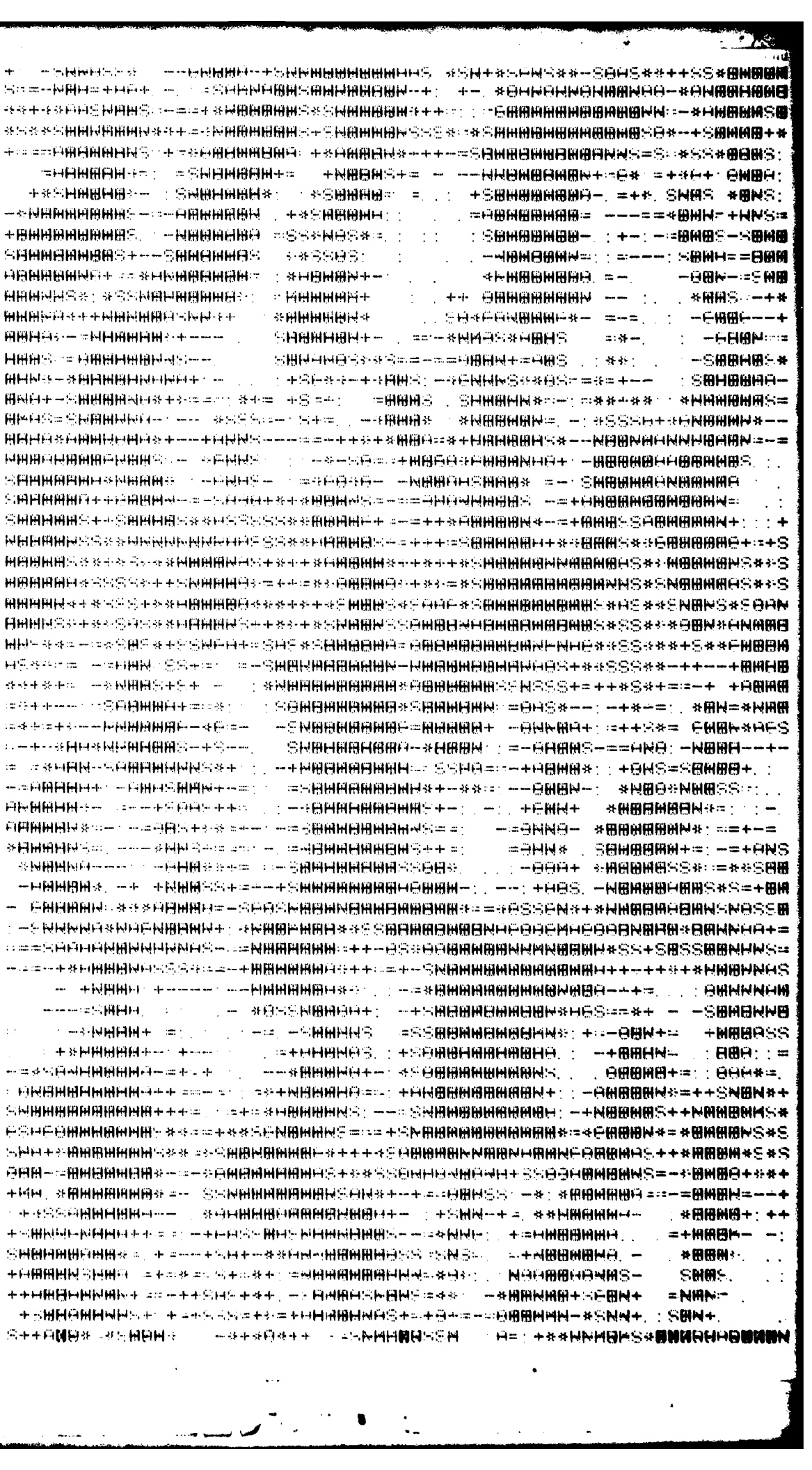

Fig. 1b
Subimage 9

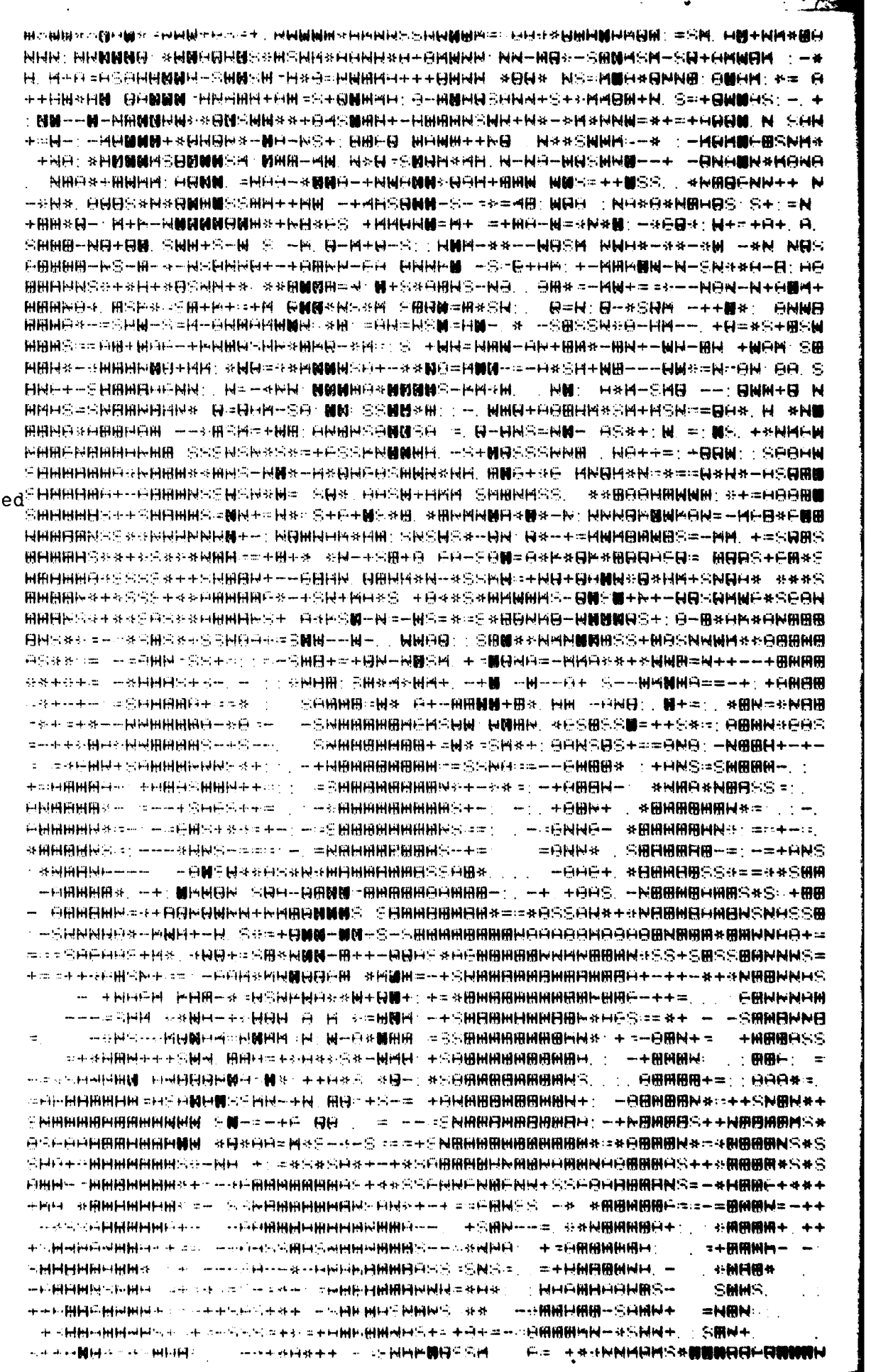

Fig. 1c
Constructed
Subimage

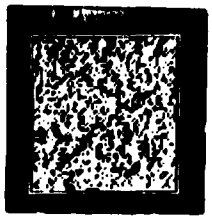

Fig. 2a Subimage 5 (above) in two-level display and histogram of the subimage (right). There are 16 levels in the original image.

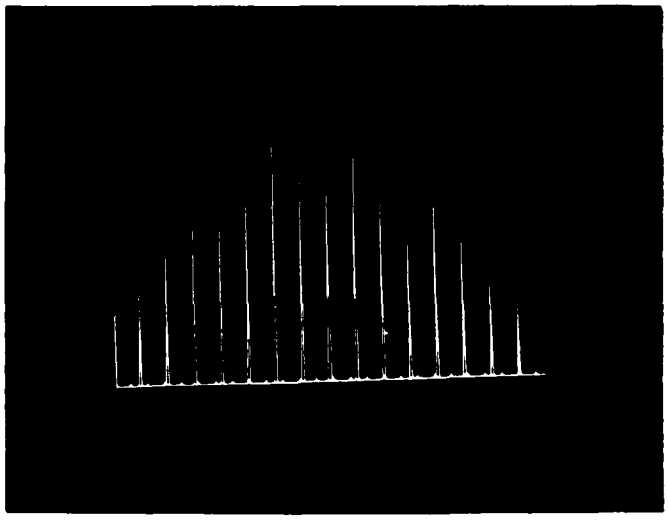

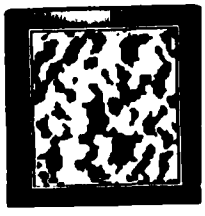

Fig. 2b Subimage 9 (above) in two -level display and histogram of the subimage (right).

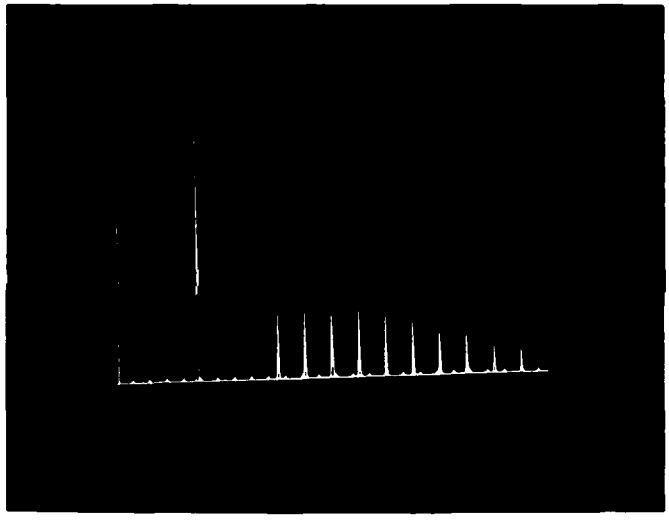

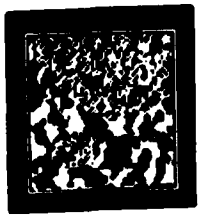

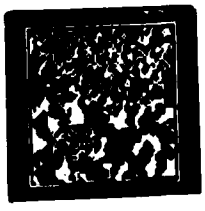

Fig. 2c Subimage constructed (two shown above) and the histogram of the constructed image (right).

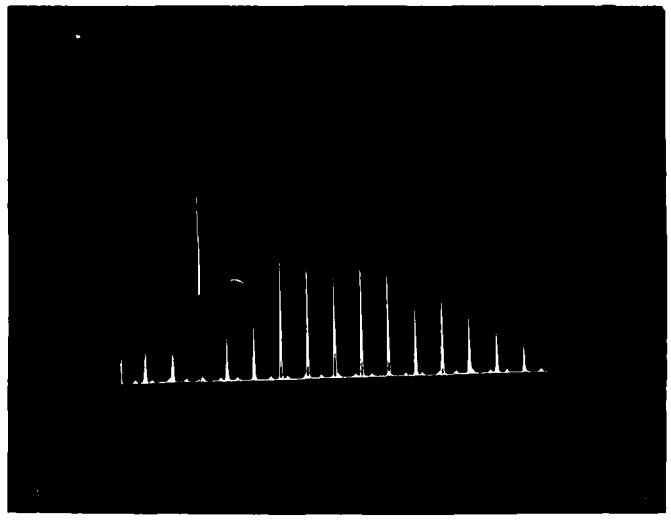

3. The Maximum Likelihood Estimation

By assuming a first-order autoregressive model, we followed closely the mathematical development in Ref. 2. The maximum likelihood estimate for the regions is obtained by the minimization of the espression (10) in Ref. 2. Fig. 4 shows the maximum likelihood (ML) segmentation obtained by assigning pixels to white and black texture type 1 and 2 respectively. This result is very close to Fig. 2 (b) of Ref. 2 which employed a higher order autoregressive model as described in the previous section. Our first-order model made use of our earlier work reported in Ref. 3.

4. The Maximum a Posteriori Estimation

The maximum a posteriori estimation which uses the combination of the Markov chain with a Gaussian autoregressive process is to minimize the expression (11) in Ref. 2. To begin with, the image segmentation is considered as an assignment of the pixels to 0 and 1. Such an assignment for a point (n, m) is referred to as its "state". The state interdependence complicates the computation of the estimate and an iterative procedure must be employed. The transition probability that plays a major role in the maximum a posteriori (MAP) segmentation is counted from the numbers of state assignment of 0 and 1 for a 5x5 neighborhood. It is noted that MAP segmentation starts with the ML segmentation result. For clarity the sequence of lineprinter outputs is shown in Fig. 5. They include the ML segmentation (Fig. 5a), Iteration 1 (Fig. 5b), Iteration 4 (Fig. 5c), Iteration 7 (Fig. 5d) and Iteration 11 (Fig. 5e). At Iteration 11, the small false region in the upper left corner starts to disappear. It is noted that such false region was not

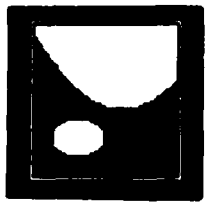

Fig. 3 Ideal segmentation

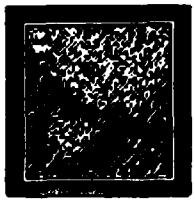

Fig. 4 ML segmentation

Fig. 6a MAP segmentation with 14 iterations

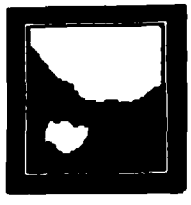

Fig. 6b Smoothing of Fig. 6a

Note: Learning samples for ML and MAP segmentations are based on 480 pixels selected from each type of texture. The following are parameters computed for each texture. Type 1 has mean of 108 and Type 2 has mean of 81.

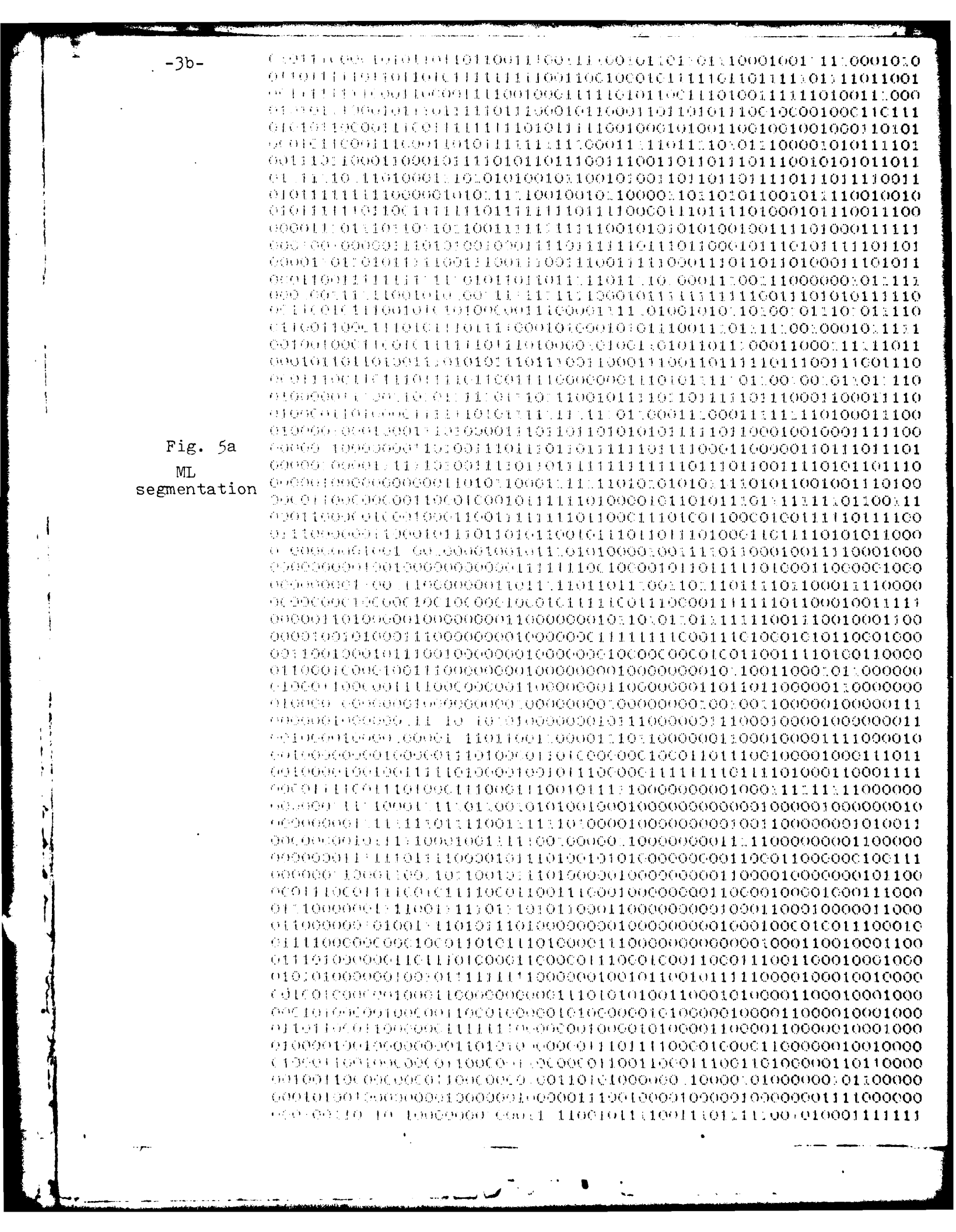

Fig. 5a
ML
segmentation

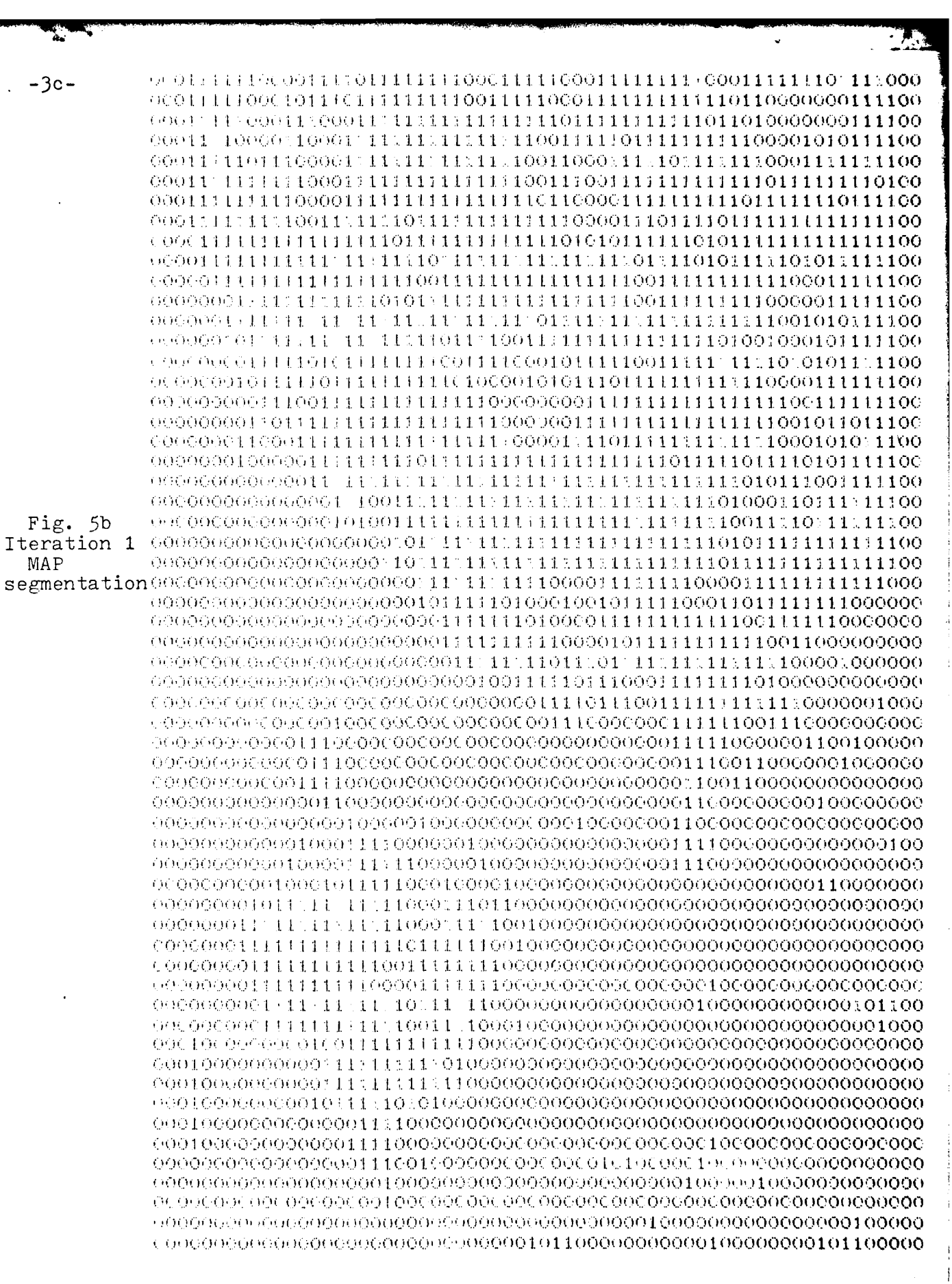

Fig. 5b
Iteration 1
MAP
segmentation

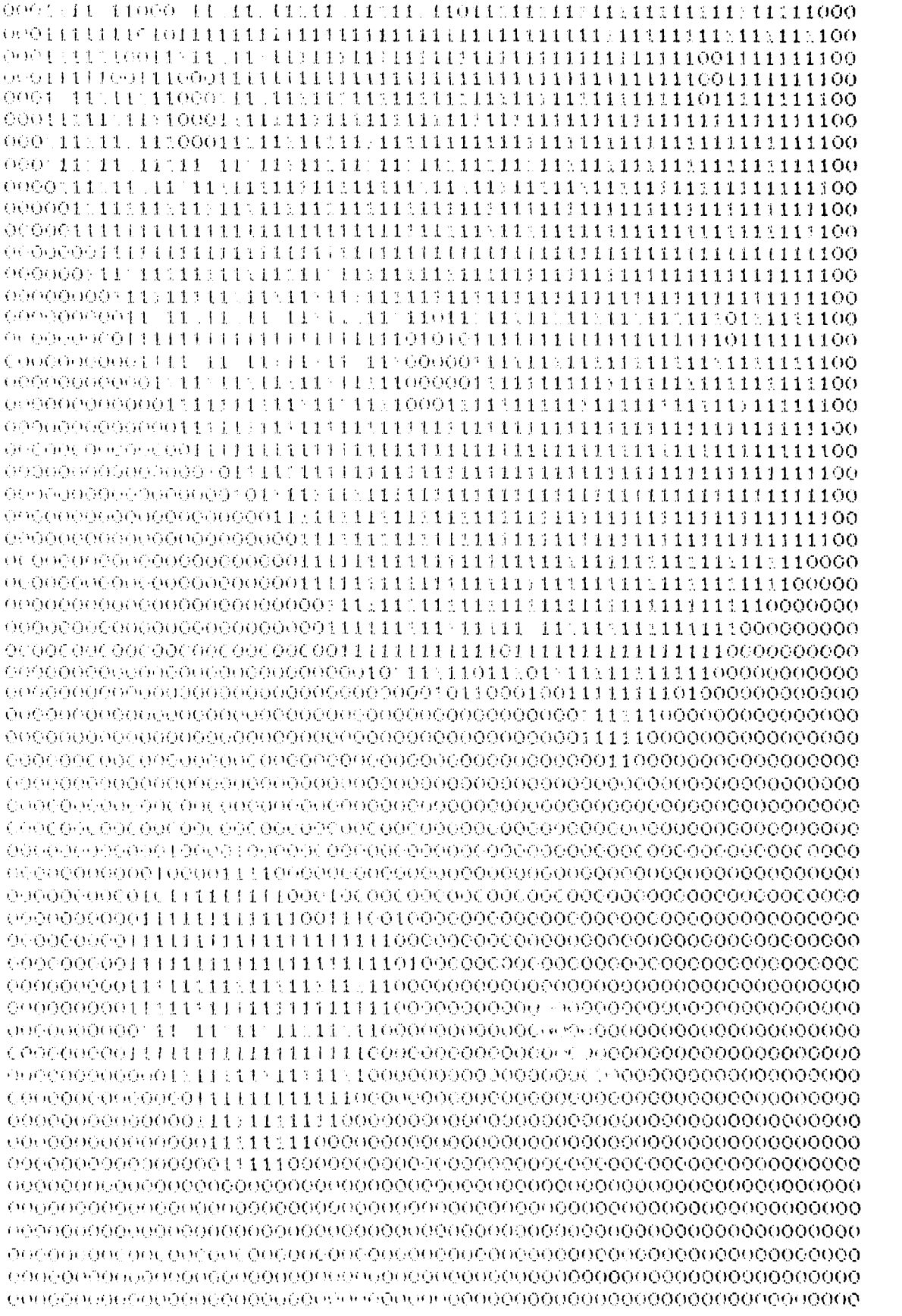

Fig. 5c
Iteration 4
MAP
segmentation

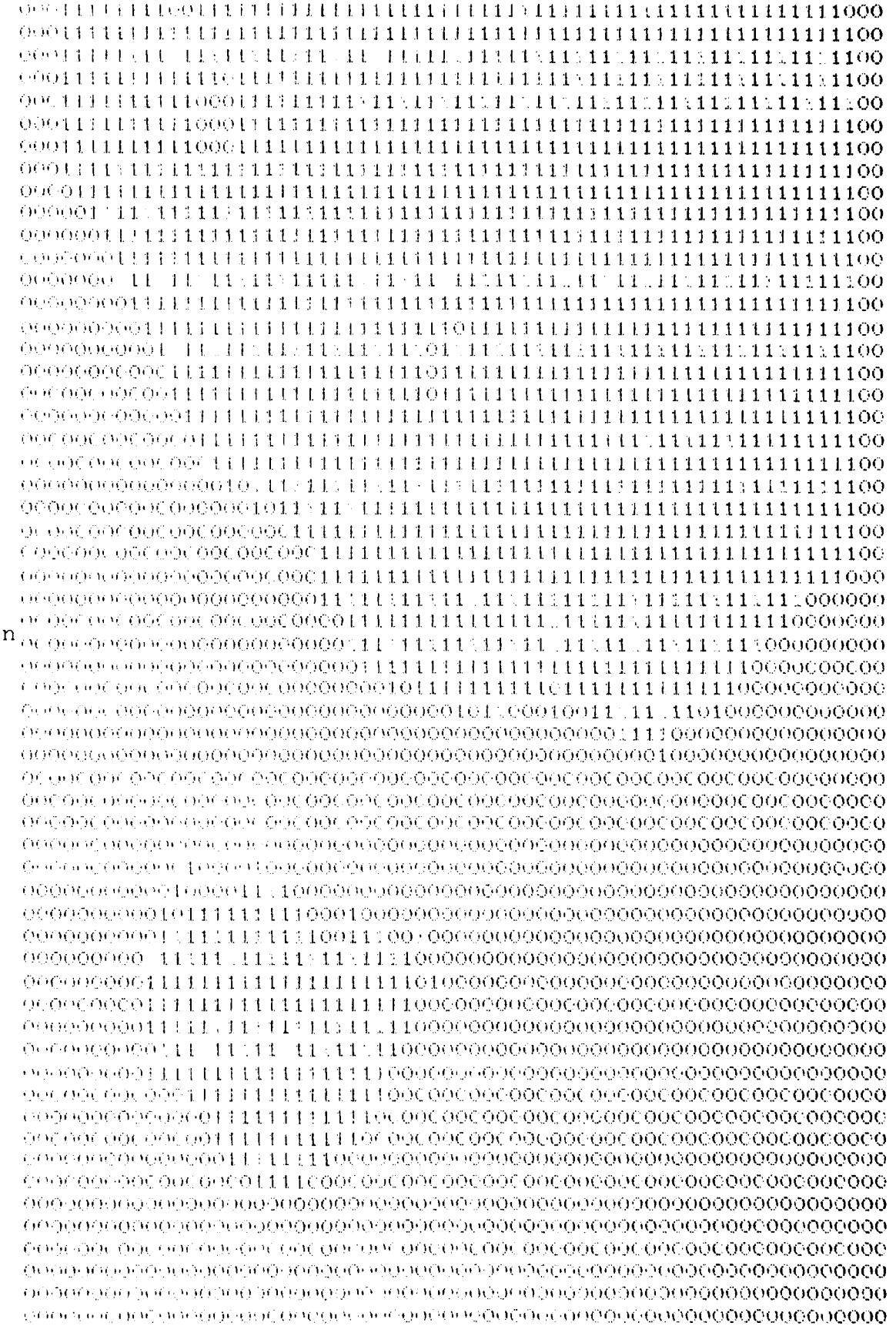

Fig. 5d
Iteration 7
MAF
segmentation

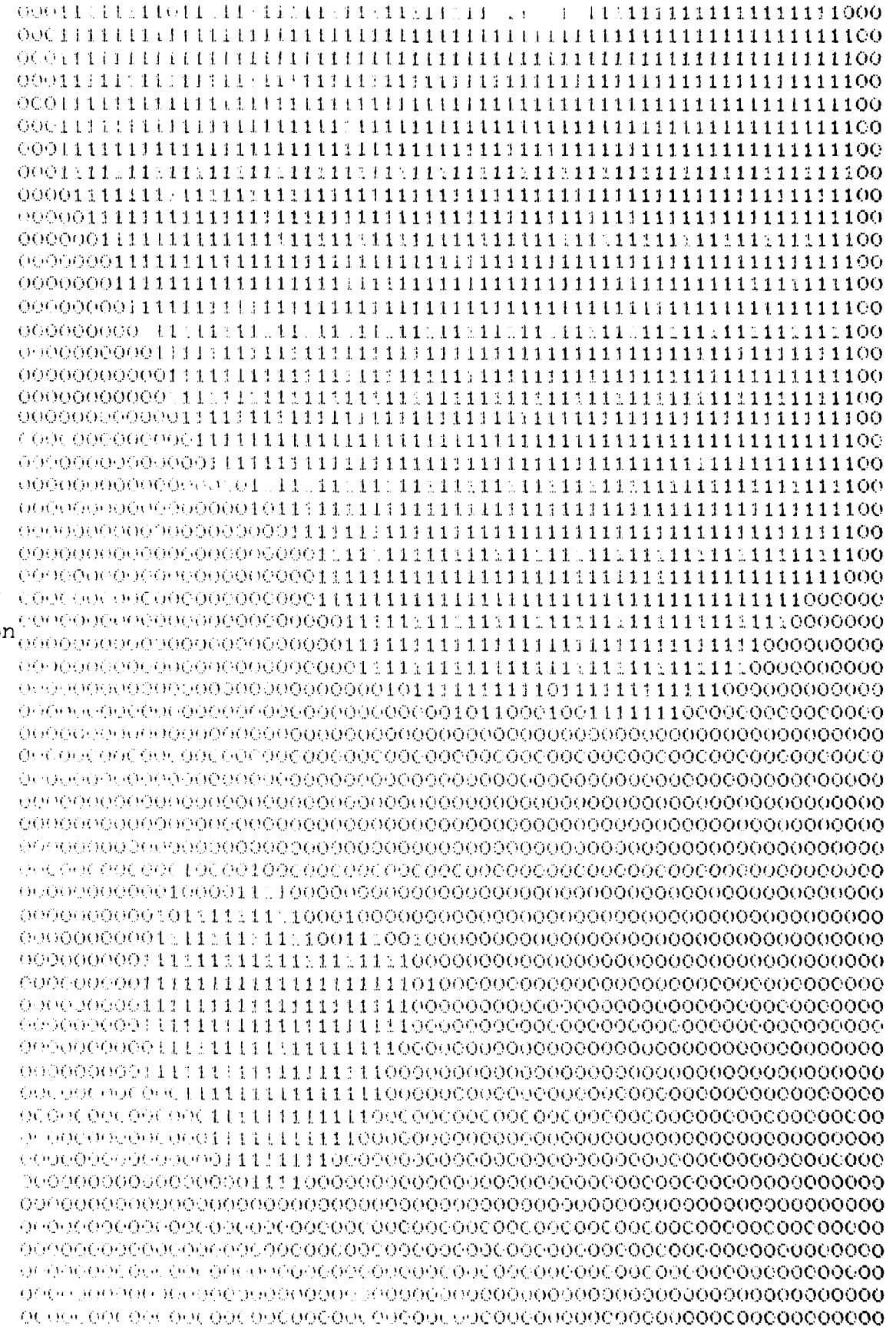

Fig. 5e
Iteration 11
MAP
segmentation

removed in Ref. 2 even after 16 iterations. At Iteration 14, the Tektronix display is shown in Fig. 6a which is then smoothed by using a procedure due to Sklansky with the result shown in Fig. 6b. The percentage segmentation error of Fig. 6b is computed as 3.96%. It is important to note that for all linear estimation methods considered in this report, the supervised learning samples are selected from regions of type 1 and type 2.

5. Fisher's Linear Discriminant

Our initial effort of using Fisher's linear discriminant follows the procedure employed in Ref. 4. The features are the gray levels of the pixels. Fig. 7a is a tabulation of the scattered matrices for Type 1(target) and Type 2 (background) textures. The two scatter matrices are nearly proportional by a factor of 3. The Fisher's linear discriminant simply cannot classify the two types of textures. A new feature selection procedure is used that extracts three features x(i), i=1,2,3 for a 3x3 neighborhood

A	B	C
D	E	F
G	H	I

by computing

$x(1) = E$

$x(2) = (A+B+C+D+E+F+G+H+I)/9$

$x(3) = (B+D+F+H) - 4E$

The learning samples are taken from a 24x28 area with each type of texture region. With each 3x3 neighborhood represented by the feature vector (x(1), x(2), x(3)), the two scatter matrices as tabulated in Fig. 7b are quite different. The Fisher's linear discriminant can then successfully segment the subimage as shown in

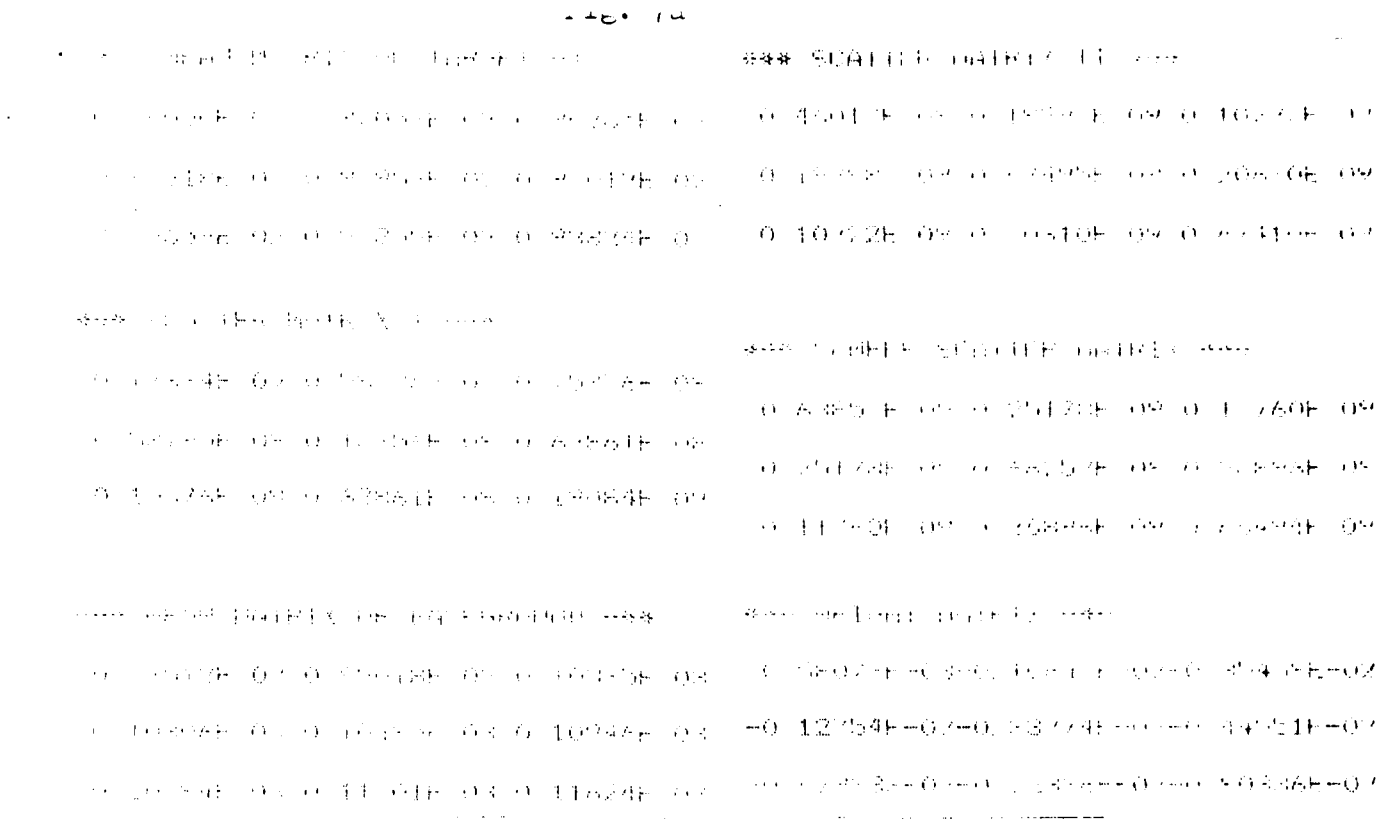

Fig. 7b

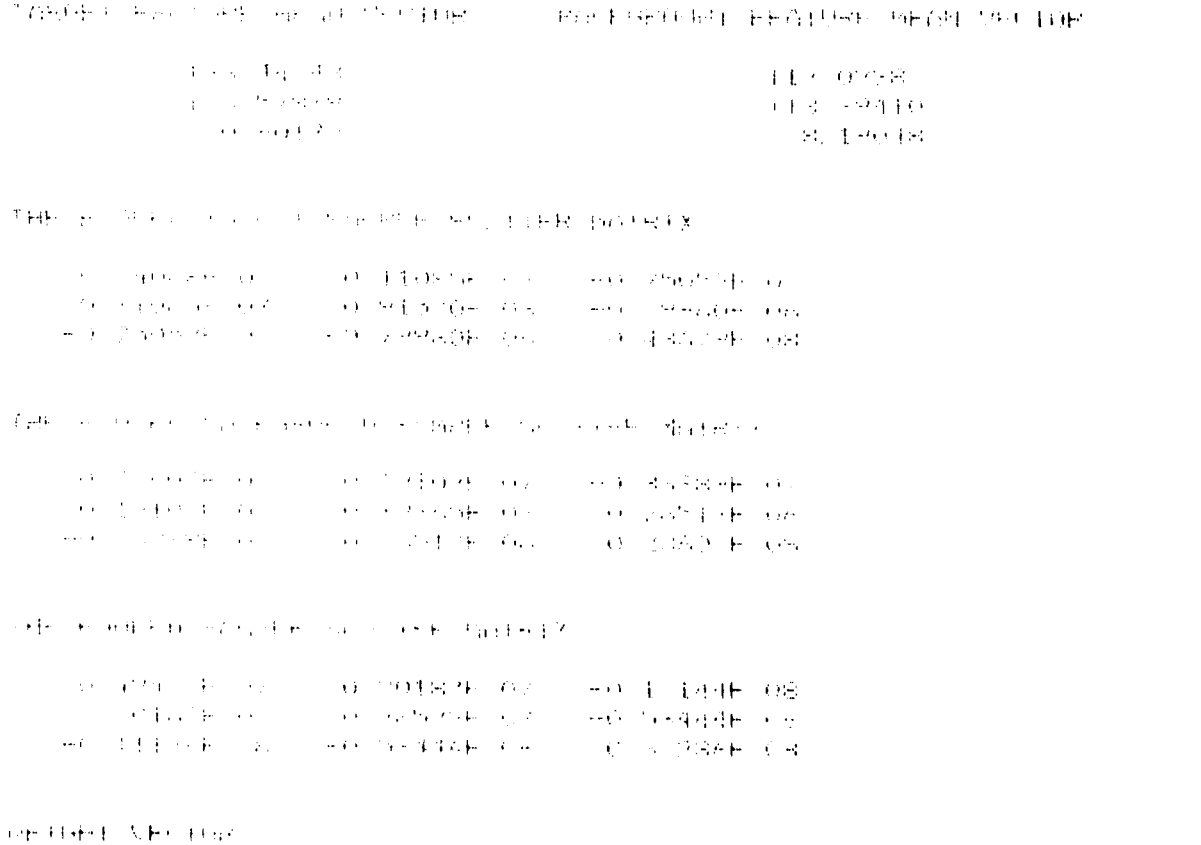

Fig. 8a Segmentation by Fisher's linear discriminant

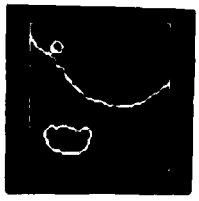

Fig. 8b Sobel gradient operation on Fig. 8a. (threshold is 3.162)

Fig. 8c Robert gradient operation on Fig. 8a. (threshold is 1)

Fig. 8a. The small false region, however, cannot be removed. The results of Sobel and Robert gradient operations on Fig. 8a are shown in Fig. 8b and Fig. 8c respectively. Due to the false region, the percentage segmentation error of Fig. 8a is 4.64%. The Fisher's linear discriminant requires slightly more computation time because of the scatter matrix and feature projection computations.

As a concluding remark, it is interesting to note that while both the maximum a posteriori estimation and the Fisher's linear discriminant are feasible linear estimation methods for image analysis, they employ quite different procedures for utilizing the statistical contextual information.

Acknowledgment We thank Dr. Therrien for helpful communications. The results reported in Sections 3 and 4 are due to R. H. Wu and the results reported in Section 5 are due to C. Yen.

References

1. C. H. Chen, "A comparative evaluation of statistical image segmentation techniques," Technical Report SMU-EE-TR-81-3, January 1981.

2. C. W. Therrien, "Linear filtering models for texture classification and segmentation," Proc. of the 5th International Conference on Pattern Recognition, pp. 1132-1135, Dec. 1980.

3. C. H. Chen and J. Chen, "A comparison of image enhancement techniques," Technical Report SMU-EE-TR-8, Dec. 1979. Also appeared in the Proc. of 1980 IEEE International Conference on Cybernetics and Society.

4. C. H. Chen and C. Yen, "Statistical image segmentation using Fisher's linear discriminant," submitted for publication, 1980.

Unclassified

SECURITY CLASSIFICATION OF THIS PAGE (When Data Entered)

REPORT DOCUMENTATION PAGE	READ INSTRUCTIONS BEFORE COMPLETING FORM
1. REPORT NUMBER	2. GOVT ACCESSION NO. AD-A094281	3. RECIPIENT'S CATALOG NUMBER
4. TITLE (and Subtitle) Some Experimental Results on Linear Estimation for Image Analysis.	5. TYPE OF REPORT & PERIOD COVERED Technical Report,
	6. PERFORMING ORG. REPORT NUMBER SMU-EE-TR-81-4
7. AUTHOR(s) C. H. Chen, Ron-Hwang Wu, Chihsung Yen	8. CONTRACT OR GRANT NUMBER(s) N00014-79-C-0494
9. PERFORMING ORGANIZATION NAME AND ADDRESS Electrical Engineering Department Southeastern Massachusetts University North Dartmouth, MA 02747	10. PROGRAM ELEMENT, PROJECT, TASK AREA & WORK UNIT NUMBERS NR 042-422
11. CONTROLLING OFFICE NAME AND ADDRESS Statistics and Probability Program Office of Naval Research, Code 436 Arlington, VA 22217	12. REPORT DATE 28 Jan 1981
	13. NUMBER OF PAGES 19
14. MONITORING AGENCY NAME & ADDRESS (if different from Controlling Office)	15. SECURITY CLASS. (of this report) Unclassified
	15a. DECLASSIFICATION/DOWNGRADING SCHEDULE

16. DISTRIBUTION STATEMENT (of this Report)

APPROVED FOR PUBLIC RELEASE: DISTRIBUTION UNLIMITED.

17. DISTRIBUTION STATEMENT (of the abstract entered in Block 20, if different from Report)

18. SUPPLEMENTARY NOTES

19. KEY WORDS (Continue on reverse side if necessary and identify by block number)

Maximum likelihood estimation
Maximum a posteriori estimation
Transition probability
Fisher's linear discriminant

20. ABSTRACT (Continue on reverse side if necessary and identify by block number)

Based on a constructed textured subimage, an experimental comparison is made on the three linear estimation methods for image segmentation, namely the maximum likelihood estimation, the maximum a posteriori estimation and the Fisher's linear discriminant. The last two methods are shown to be feasible for effective image segmentation.

DD FORM 1473 EDITION OF 1 NOV 65 IS OBSOLETE

S/N 0102-LF-014-6601

407932

SECURITY CLASSIFICATION OF THIS PAGE (When Data Entered)

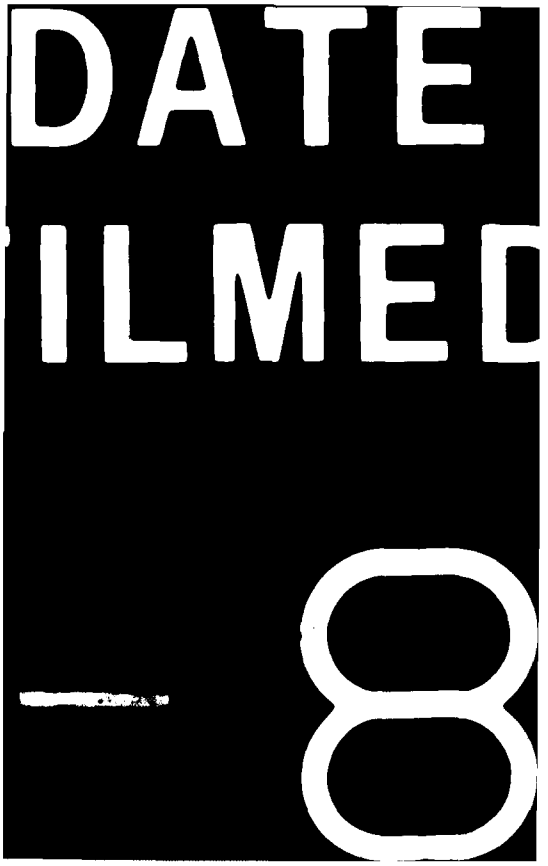
DATE
ILMED
8